PROTEINS
STRUCTURE ■ FUNCTION ■ BIOINFORMATICS

Gain of local structure in an amphipathic peptide does not require a specific tertiary framework

Ernesto A. Roman,[1] Pablo Rosi,[1] Mariano C. González Lebrero,[1] Rodolfo Wuilloud,[2] F. Luis González Flecha,[1] José M. Delfino,[1] and Javier Santos[1,3]*

[1] Department of Biological Chemistry and Institute of Biochemistry and Biophysics (IQUIFIB), School of Pharmacy and Biochemistry, University of Buenos Aires, Junín 956, C1113AAD, Buenos Aires, Argentina

[2] Laboratory of Environmental Research and Services of Mendoza (LISAMEN), CCT-CONICET Mendoza. Av. Ruiz Leal S/N Parque General San Martín, M 5502 IRA Mendoza, Argentina

[3] Department of Science and Technology, University of Quilmes, Roque Sáenz Peña 352, B1876XD, Bernal, Argentina

ABSTRACT

In this work, we studied how an amphipathic peptide of the surface of the globular protein thioredoxin, TRX94-108, acquires a native-like structure when it becomes involved in an apolar interaction network. We designed peptide variants where the tendency to form α-helical conformation is modulated by replacing each of the leucine amino acid residues by an alanine. The induction of structure caused by sodium dodecyl sulfate (SDS) binding was studied by capillary zone electrophoresis, circular dichroism, DOSY-NMR, and molecular dynamics simulations (MDS). In addition, we analyzed the strength of the interaction between a C18 RP-HPLC matrix and the peptides. The results presented here reveal that (a) critical elements in the sequence of the wild-type peptide stabilize a SDS/peptide supramolecular cluster; (b) the hydrophobic nature of the interaction between SDS molecules and the peptide constrains the ensemble of conformations; (c) nonspecific apolar surfaces are sufficient to stabilize peptide secondary structure. Remarkably, MDS shed light on a contact network formed by a limited number of SDS molecules that serves as a structural scaffold preserving the helical conformation of this module. This mechanism might prevail when a peptide with low helical propensity is involved in structure consolidation. We suggest that folding of peptides sharing this feature does not require a preformed tightly-packed protein core. Thus, the formation of specific tertiary interactions would be the consequence of peptide folding and not its cause. In this scenario, folding might be thought of as a process that includes unspecific rounds of structure stabilization guiding the protein to the native state.

Proteins 2010; 78:2757–2768.

Key words: thioredoxin; SDS; helical propensity; leucine pair of interactions; molecular dynamics simulations; secondary structure stability; folding.

INTRODUCTION

A glance at the sequence of a protein does not directly reveal the existence of structure. However, it encrypts the physicochemical properties needed to assemble itself into a three-dimensional arrangement.[1] A straightforward example that illustrates how a sequence determines a structure is the case of natural amphipathic α-helices. The amphipathicity of an α-helix is a property that becomes manifest in the folded conformation. Amphipathic α-helices occur ubiquitously in globular proteins where they simultaneously interact on one face with water molecules and on the opposite face with other residues of the hydrophobic core. In general, local (near in sequence) and tertiary interactions contribute together to attain structure. Nevertheless, even for this deceivingly simple case, we do not know about the relative weight and complex relationship between these two classes of interactions to provide stability to this structural module. For example, the grafting of nonhomologous amphipathic α-helices into β-lactamase results in native-like states highlighting the robustness of the folding process.[2] On the other hand, despite the presence of stabilized individual helices, defects in the acquisition of native-like packing were observed for a de novo designed triple-helix bundle.[3] Furthermore, protein structure seems to balance both thermodynamic stability and conformational specificity toward the folded state over the ensemble of unfolded/partially folded conformations. An excellent example is the family of α-2 dimeric four-helix bundle, and

Additional supporting information may be found in the online version of this article.
Grant sponsors: Agencia Nacional de Promoción Científica y Tecnológica (ANPCyT), Consejo Nacional de Investigaciones Científicas y Técnicas (CONICET), Universidad de Buenos Aires (UBACyT), Universidad Nacional de Quilmes (UNQ); Grant sponsor: ANPCyT; Grant number: PME2003-0026.
Ernesto A. Roman and Pablo Rosi contributed equally to this work.
*Correspondence to: Javier Santos, Department of Biological Chemistry and Institute of Biochemistry and Biophysics (IQUIFIB), School of Pharmacy and Biochemistry, University of Buenos Aires, Junín 956, C1113AAD, Buenos Aires, Argentina.
E-mail: jsantos@qb.ffyb.uba.ar.
Received 11 February 2010; Revised 18 May 2010; Accepted 20 May 2010
Published online 8 June 2010 in Wiley Online Library (wileyonlinelibrary.com).
DOI: 10.1002/prot.22789

particularly, the designed protein α-2D with perfectly defined tertiary structure, in which fine-tuned interactions also contribute to a uniquely folded state.[4]

Tertiary contacts established between amphipathic modules and the rest of the protein may be mimicked *in vitro* by interactions with apolar surfaces and amphiphiles, for example, reverse phase C18,[5] sodium dodecyl sulfate (SDS),[6] or 2,2,2-trifluoroethanol (TFE).[7,8] An important issue here is to establish whether these interactions (a) select and stabilize the α-helical structure from the vast space of conformations or (b) induce structure by the stabilization of a nucleation site, followed by a propagation of the α-helix. In any case, the reduced conformational freedom of the bound peptide might anticipate the further precise packing of amino acid side chains found in the core of the native state. In particular, detergents, such as SDS display a dual action because they are able to act as unfolding agents,[9] by disrupting key core interactions, but by the same token, they are able to induce and stabilize secondary structure.[10,11]

Recently, in a complementation experiment between a partially folded protein fragment (TRX1-93) and a random coil peptide (TRX94-108) derived from *E. coli* thioredoxin (TRX), we demonstrated that it is possible to attain a native-like structure.[12] We also showed that residues L99 and L103 are crucial for the consolidation of the tertiary structure of the complex between TRX1-93 and TRX94-108. Interestingly, these residues are also critical for the stabilization of the helical structure that the peptide TRX94-108 adopts in TFE solution.[13]

Our aim here is to investigate how the amphipathic peptide TRX94-108 adopts a stable structure, with emphasis in the analysis of the specificity requirements of the phenomenon provided by its own sequence and the folding environment. To this end, the approach involves both *in vitro* studies and molecular dynamics simulations (MDS). We experimentally characterized the acquisition of native-like structure of TRX94-108 as a consequence of the interaction between the peptide and apolar milieu (detergent molecules or modified solid state surfaces). Circular dichroism (CD) spectroscopic evidence points to the stabilization of a helical conformation induced and preserved in the presence of SDS. MDS support this fact and highlight the role played by particular apolar residues that make contacts with the detergent molecules. In the same vein, the induction of a helix is also observed in the presence of preformed long-chain aliphatic surfaces. In the context of full-length proteins, we hypothesize that the interaction of amphipathic peptides with emerging apolar surfaces originated by the folding of the rest of the polypeptide chain would suffice to restrain the conformational space available to the peptide. In this fashion, secondary structure stabilization of this module would signify a momentous step driving further specific interactions with the rest of the protein, and ultimately leading to the consolidation of the native state.

METHODS

General details

Peptide TRX94-108, of sequence LSKGQLKEFLDANLAY, was synthesized and partially purified by GenScript Corp. The purification was completed by HPLC (Rainin Dynamax, NY) using a reverse phase C18 semipreparative column equilibrated in 0.05% aqueous TFA. TRX94-108 was eluted with a linear gradient from 30 to 45% aqueous acetonitrile (ACN), 0.05% TFA; the peptide typically elutes at 40% ACN. Fractions containing >98.0% pure peptide were pooled and lyophilized. Stock aqueous solutions of peptide were prepared up to 1.5 m*M* concentration. The experiments were carried out in 2.0 m*M* sodium phosphates, pH 7.0, unless other experimental conditions are specified.

The same procedure was carried out in the case of mutant peptides: L94A, L99A, L103A, and L107A and a scrambled nonhelical peptide (NHP) of the same composition as the wild-type peptide and the following sequence: LDLKSGQLKAENAYFL. The main feature of this peptide is that it shows almost no propensity to form secondary structure, as predicted by AGADIR.[14–17] The mean hydrophobicity and the hydrophobic moment of peptides were calculated with an ad hoc Excel spreadsheet embedded with a macro that calculates those magnitudes from an input of 3D backbone coordinates in pdb format and the Fauchere and Pliska hydrophobicity scale.[18] In addition, we prepared the amphipathic helical peptides: FXN H2 (SLHELLAAELTKALKY), comprising residues 181–195 of human frataxin[19] and peptide PA2 (TLLAQIVKLVEDAMGY), comprising residues 312–326 of the soluble actuator domain of *Archaeoglobus fulgidus* CopA.[20] Where appropriate, a C-terminal tyrosine tag was added to allow the measurement of concentration by absorbance in the near-UV region (using an extinction coefficient: $\varepsilon_{280\ \mathrm{nm}} = 1{,}490\ \mathrm{M}^{-1}\ \mathrm{cm}^{-1}$). The mass of peptides was checked by HPLC/ESI-MS using a 1.0 mm × 30 mm Vydac C8 column, eluted at a flow rate of 40 μL/min, in a Surveyor HPLC system connected online to an LCQ Duo (ESI ion trap) mass spectrometer (Thermo Finnigan, San José, CA).

Adsorption of peptides to C18 surfaces

Stock peptide solutions were diluted in 20 m*M* sodium phosphates, pH 7.0 to a final concentration of 10.0 μ*M*. Samples were injected in an analytical C18 RP-HPLC chromatography column previously equilibrated in 5 m*M* sodium phosphates, pH 7.0. The elution solvent was 5 m*M* sodium phosphates, pH 7.0/ACN 70%. The gradient was 0–60% ACN in 30 min. Peak elution was followed by absorption at 215 nm, using a UV detector (Rainin Dynamax) connected online to the column. Experiments were performed at room temperature. In addition, we evaluated binding of peptides to C18-alkyl-

modified quartz plates, as described by Blondelle *et al.*[21] Briefly, each plate was washed with concentrated sulfuric acid for 40 min at 75°C. Then, they were washed with water and acetone, and dried under vacuum. After that, quartz plates were treated with 1*M* octadecyl trichloro silane (Aldrich, Milwaukee, WI) in anhydrous heptane for 24 h at room temperature in an evacuated desiccator over potassium hydroxide. To complete the C18 modification, plates were incubated at 60°C with octadecan-1-ol for 24 h. Finally, modified quartz plates were washed by sonication in anhydrous methanol at room temperature and dried under vacuum.

Circular dichroism spectroscopy

Ellipticity of samples was evaluated using a Jasco 810 spectropolarimeter. Far-UV CD spectra were recorded in the range between 185–250 nm. A cell of 0.1 cm was used and data was acquired at a scan speed of 20 nm/min. At least three scans were averaged for each sample. Blank scans were subtracted from the spectra and values of ellipticity were expressed in units of deg cm^2 $dmol^{-1}$. Peptide concentration was 100 μ*M*, unless expressed otherwise in the text. Structure induction by SDS was achieved by additions from a stock detergent solution (15 m*M*). Theoretical calculation of ellipticity for a 100% helical peptide was performed as explained by Luo and Baldwin.[7] In addition, we measured the ellipticity of peptides bound to C18-alkyl-modified quartz plates.

Critical micelle concentration

Although critical micelle concentration (CMC) for SDS has been previously reported, we checked the CMC under the experimental conditions used in this work: 2.0 m*M* sodium phosphates, pH 7.0, because this parameter is highly modulated by the ionic strength.[22] Determinations were carried out using 8-anilino-1-naphthalene sulfonic acid (ANS).[23] If ANS is surrounded by a polar medium, the quantum yield of fluorescence is low with an emission maximum around 520 nm. However, as micelles form, ANS fluorescence increases and a blue shift occurs to around 480 nm, as a consequence of the interaction of ANS with the nonpolar environment.[24,25] Briefly, a solution of 50.0 μ*M* ANS was prepared in 2.0 m*M* sodium phosphates, pH 7.0. Next, detergent was added in small aliquots and fluorescence spectra were recorded using an Aminco Bowman Series II spectrofluorometer. Total fluorescence intensity was corrected by dilution and plotted against detergent concentration. The CMC is the concentration where the slope shifts abruptly. The same general procedure was followed to measure the CMC of SDeS.

Capillary zone electrophoresis

We used capillary zone electrophoresis (CZE) to determine the binding of SDS molecules to the peptides.[26] The CZE equipment was a Beckman Coulter (Fullerton, CA) P/ACE MDQ, with a UV/Vis diode array detector and a sample/capillary thermostatization system. Routine measurements were obtained by using a 75 μm (inner diameter) and 375 μm (outer diameter) fused-silica capillary obtained from MicroSolv Technology Corp. (Eatontown, NJ), having a total length of 67 cm and a length to the observation window of 59 cm. The buffer used was 2.0 mM sodium phosphates, pH 7.0. Samples were pressure-injected at the anodic side at 0.50 psi for 5 s. All experiments were carried out at 25°C, using a constant voltage of 20 kV. These conditions generated a current of 4.9 μA (0.0 mM SDS), 7.0 μA (2.0 mM SDS), and 10.5μA (5.0 mM SDS). Electropherograms were obtained by continuous monitoring of the absorption in the range 190–315 nm at the observation window. SDS is transparent in this region of the UV spectrum.

The charge of SDS/TRX94-108 supramolecular cluster was calculated from its electrophoretic mobility μ as in,[27] by using the equation:

$$\mu = \frac{eZ \cdot f(\kappa R_h)(1 + \kappa R_h)}{6\pi\eta R_h[1 + \kappa(R_h + r_b)]} \quad (1)$$

where R_h is the hydrodynamic radius, e is the electron charge (-1.602×10^{-19} C), Z is the valence, κ is the inverse of the Debye-Hückel screening length, η is the dynamic viscosity of water at 25°C (0.00089 N m^{-2} s), r_b is the average radius of a buffer ion, $f(\kappa R_h)$ is the value of the Henry function for κR_h.

Determination of hydrodynamic radius

The hydrodynamic radius (R_h) of the isolated TRX94-108 and the SDS/peptide supramolecular cluster in 2.0 m*M* sodium phosphates, 5.0 m*M* SDS, pH 7.0 (0.2 m*M*, peptide concentration) was determined by diffusion order spectroscopy NMR (DOSY-NMR).[28] Spectra were acquired on a Bruker Avance 600 MHz spectrometer. Data acquisition for pulsed-field gradient (PFG) NMR experiments was carried out at 25°C on unlabeled TRX94-108, dissolved in D_2O and containing dioxane as an internal radius standard (2.12 Å) and viscosity probe. A series of 20 1D spectra were collected as a function of gradient amplitude. The gradient strength was shifted from 0.67 to 32.03 G cm^{-1} in a linear manner. Diffusion coefficients for dioxane ($D_{dioxane}$) were 1.057×10^{-9} m^2 s^{-1} in the absence of SDS and 1.032×10^{-9} m^2 s^{-1} in the presence of 5.0 m*M* SDS. The R_h of the peptides was calculated using equation:

$$R_{h_{TRX94-108}} = \frac{D_{dioxane}}{D_{TRX94-108}} \times R_{h_{dioxane}} \quad (2)$$

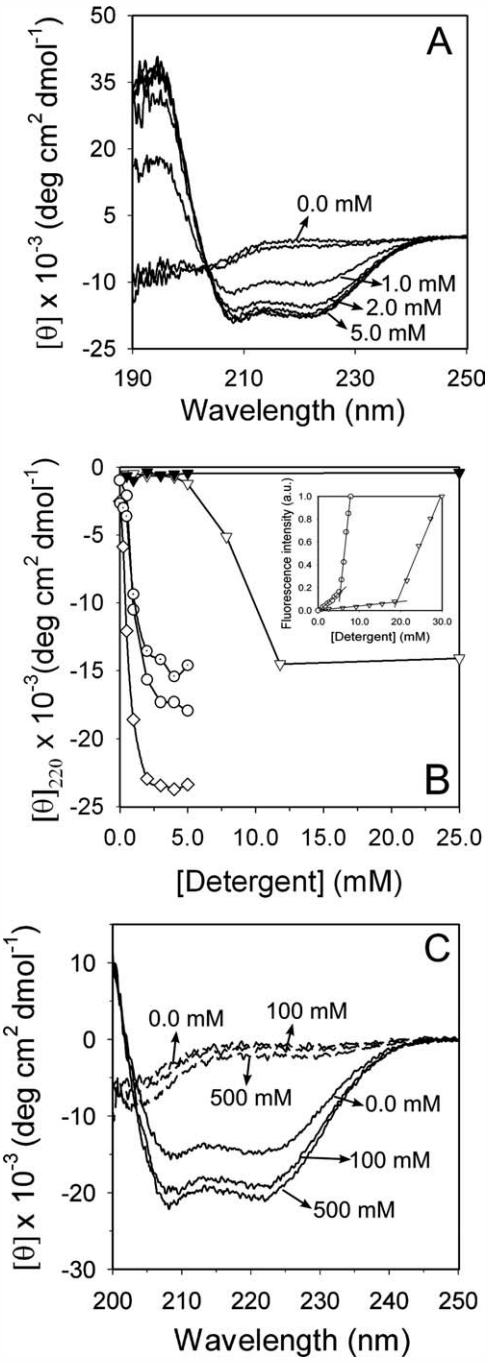

Figure 1

Induction of α-helix structure by SDS. (**A**) CD spectra corresponding to TRX 94-108 with 0.0, 0.5, 1.0, 2.0, 3.0, 4.0, and 5.0 m*M* SDS. (**B**) Induction of α-helix structure of TRX 94-108 by detergents of different apolar tail length. SDS (○), SDeS (▽), and SPS (▼). Helical induction of FXN H2 (Θ), PA2 (◊) peptides by SDS are also plotted. Inset shows the CMC determination for SDS (○) and SDeS (▽) as the change in the total fluorescence intensity upon micelle formation. (**C**) Effect of the ionic strength in the induction of α-helix structure. CD spectra corresponding to TRX 94-108 after addition of 0, 100, and 500 m*M* NaCl in the absence (dotted lines) and in the presence of 2 m*M* SDS (solid lines) are shown.

Molecular dynamics simulations

MDS were carried out with GROMACS 3.3[29] and GROMOS 53a6 force field,[30] to investigate the conformational landscape of TRX94-108 in solution or complexed with one to six SDS molecules, or with four, six, or eight molecules of sodium pentyl sulfate (SPS) per peptide. The molecular parameters for the SDS and SPS were obtained via the PRODRG 2 program[31] and their initial structures were modeled as extended conformations. The simulations were performed in a 5 nm-cubic box with periodic boundary conditions. The system was simulated as an isobaric-isothermal ensemble at 300 K and 1 bar, using weak temperature and pressure coupling (0.1 and 1.0 ps^{-1}, respectively).[32] In all cases, the initial structures were extracted from the 3D coordinates of chain A of the crystallographic structure, PDB ID: 2TRX.[33] The SDS molecules (or SPS) and the Na^+ ions were added to the simulation box at random. The structure of each peptide or detergent/peptide cluster was solvated with about 5000 SPC (simple point charge) water molecules.[34] Long-range interactions were computed according to the particle mesh Ewald sum. Conditioning consisted of 5 ns of peptide position-restrained MDS. The conditioned system was the starting point for each 30 ns simulation, and the first 5 ns were discarded for the statistical analysis. In all cases, simulations were performed from two different random starting configurations of the system. We used radial distribution functions $G(r)$ to describe how the SDS atomic density varies as a function of the distance to any heavy atom of a selected residue. $G(r)$ values were calculated as described in the GROMACS 3.3 user manual.[29] Molecular graphics were prepared using VMD.[35]

RESULTS

SDS induces α-helical conformation in wild-type peptide TRX94-108

TRX94-108 dissolved in aqueous solution yields a far-UV CD spectrum compatible with random coil conformation [Fig. 1(A)]. TRX94-108 is a monomer at 200 μ*M* concentration, as evidenced by DOSY-NMR experiments ($D_{TRX94-108} = 2.283 \times 10^{-10}$ m^2 s^{-1}, the diffusion coefficient of the peptide yielding a value for R_h (10.0 ± 0.2 Å) compatible with a random coil peptide of this molecular weight). On the other hand, in the presence of 1.0–5.0 m*M* SDS, a range below its critical micelle concentration [CMC = 5.4 m*M*, Fig. 1(B), inset], the CD spectra acquire the typical signatures of α-helical conformation [Fig. 1(A)]. The transition between random coil and α-helix occurs in the mixing time of the experiment (in less than 20 s by manual mixing) and is completely reversible, as is demonstrated by subsequent dilution of the sample. The CD signal at 220 nm observed for TRX94-108 in SDS solution (−17,500 deg cm^2 $dmol^{-1}$, at 25°C and 5.0 m*M* SDS) indicates an overall α-helix content of

Table I
Biophysical Properties of Peptide Variants

Peptide	$C_{50\%}$[a] (m*M*)	$C_{m\ Urea}$[b] (M*M*)	⟨H⟩[c]	$\lvert\mu_H\rvert$[c]	$\mu^d \times 10^8$ ($m^2\ V^{-1}\ s^{-1}$)	AGADIR[e] (%)	Sequence
Wild-type	1.5	5.0	0.37	5.64	−4.36	5.5 (13.2)	LSKGQLKEFLDANLAY
L94A	3.0	2.5	0.28	5.81	−4.03	3.3 (9.0)	ASKGQLKEFLDANLAY
L99A	3.0	1.8	0.28	4.48	−4.05	2.2 (5.8)	LSKGQAKEFLDANLAY
L103A	3.0	2.0	0.28	5.27	−4.06	2.5 (5.5)	LSKGQLKEFADANLAY
L107A	2.0	2.8	0.28	5.03	−4.08	2.6 (6.0)	LSKGQLKEFLDANAAY
NHP	nd	nd	0.37	2.80	−1.72	0.9 (1.3)	LDLKSGQLKAENAYFL

[a]Is the SDS concentration necessary to achieve 50% of the effect in ellipticity change [Fig. 2(A)].
[b]Was calculated as the concentration of denaturant where half-maximal unfolding effect was reached [Fig. 2(B)].
[c]The mean hydrophobicity ⟨H⟩ and the module of the hydrophobic moment $\lvert\mu_H\rvert$ were calculated using the Fauchere and Pliska hydrophobicity scale[18] and the 3D peptide structure taken from the PDB ID: 2TRX.
[d]The electrophoretic mobility was calculated using $\mu_A = [(x/t_A) - (x/t_{EO})]/E$, where the retention time (t_A) is the time taken for the protein zone to migrate the fixed distance (x) from the point of sample application to the position in the capillary that is being monitored by the detector. t_{EO} is the retention time for the uncharged marker, acetonitrile. E, the electric field strength, is taken as the applied potential gradient divided by the total length of the capillary across which the constant voltage is applied.
[e]AGADIR helical propensity calculations were performed assuming a pH 7.0 and 0°C, and a ionic strength of 100 m*M*. Values for the N-acetylated and C-amidated are between brackets.

∼60%, by comparison with the theoretically expected value for a 16-residue peptide in this conformation (−29,250 deg cm^2 $dmol^{-1}$). Remarkably, at 5.0 mM SDS, TRX94-108 shows a R_h = 21.2 Å by DOSY-NMR ($D_{SDS/TRX94\text{-}108} = 1.013 \times 10^{-10}$ m^2 s^{-1}), a value indicative of an association between the peptide and SDS molecules (see below).

To examine the contribution of the electrostatic interactions on the acquisition of secondary structure, salt concentration was increased from 0 to 500 m*M* NaCl in a SDS/peptide solution at 2.0 m*M* SDS. An increase of 25% in the far-UV CD bands at 208 and 220 nm suggests that raising the ionic strength reduces the electrostatic repulsion among sulfate groups, and/or optimizes the hydrophobic interaction between SDS and the peptide. In the absence of SDS, a high salt concentration (500 mM) does not produce any significant change in the shape of the spectrum [Fig. 1(C)].

To evaluate the magnitude of the apolar interaction between the peptide and the hydrocarbon moiety of the detergent, we tested the induction of secondary structure with sodium decyl sulfate (SDeS) and sodium pentyl sulfate (SPS) [Fig. 1(B)]. SDeS induces α-helical structure of TRX94-108 at a significantly higher concentration than SDS, that is, the observed detergent concentrations necessary to attain 50% of the effect ($C_{50\%}$) are 9.5 m*M* and 1.5 m*M* for SDeS and SDS, respectively. On the other hand, SPS does not induce secondary structure even at concentrations as high as 50 m*M*. Altogether, these evidences point to detergent hydrophobicity as the main factor constraining the conformational ensemble of TRX94-108 in solution toward a helical form.

There are critical sequence determinants in TRX94-108 for the stability of the SDS/peptide supramolecular cluster

We designed a series of single mutants of the peptide in which the wild-type sequence is mutated at each of the leucine amino acid residues by alanine. We also designed a NHP that preserves the same amino acid composition of the wild-type peptide, but whose sequence was modified to reduce its helical tendency, as predicted by the AGADIR index (Table I). As expected, the far-UV CD spectrum of NHP is compatible with a random coil conformation up to the maximal concentration of SDS assayed (5.0 m*M*). All single amino acid mutants require higher detergent concentrations to induce secondary structure than the amount needed for wild type peptide [Fig. 2(A)]. This effect is more pronounced for peptides L99A, L103A, and L94A ($C_{50\%}$ ∼3 m*M*) than for peptide L107A ($C_{50\%}$ ∼2 m*M*). This is probably a consequence of the disruption of a stacking interaction between the former three leucine side chains, a factor that could be critical to stabilize the helical conformation. By contrast, residue L107 is placed near the C-terminus of the α-helix, a likely disordered region, therefore less prone to cause destabilization. In agreement with this interpretation, 1D NMR spectra show that signal broadening and changes in chemical shift are more pronounced in the phenylalanine aromatic signals than in the tyrosine ones (see Fig. 3). Because of the heavy resonance overlap and the presence of the intense SDS signals in the aliphatic region, no specific effect can be accurately monitored here (data not shown).

To understand the role of leucine side chains on the stability of the induced helical conformations, we studied the urea-induced unfolding of the SDS/peptide cluster in 5.0 m*M* SDS. All transitions studied (for L94A, L99A, L103A, L107A, and wild-type peptides) show cooperativity and the analysis of the $C_{m\mathrm{Urea}}$ values (the concentration of urea necessary to attain a half-maximal effect) evidences that the SDS/wild-type peptide complex is the most stable one. Particularly, the L99A and L103A clusters are greatly destabilized [Fig. 2(B)].

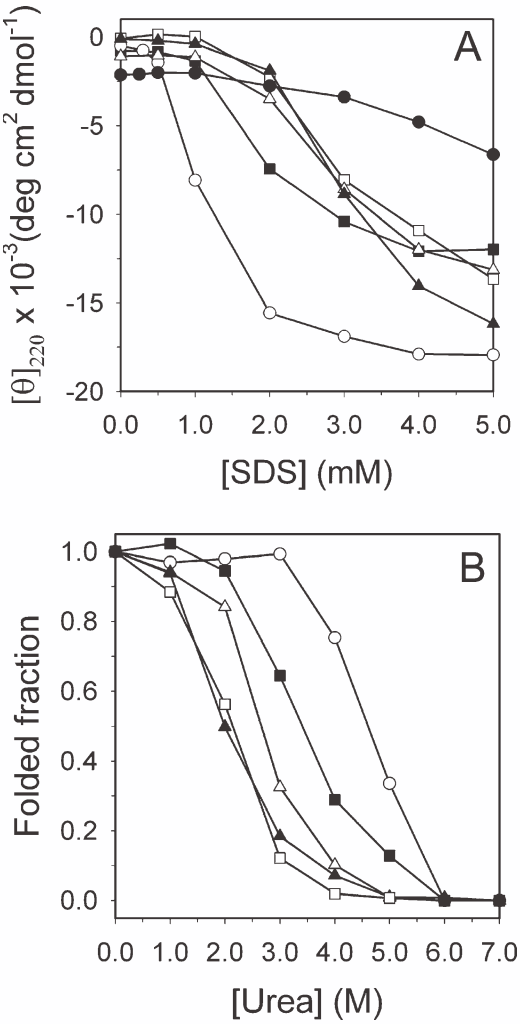

Figure 2

Effect of SDS on peptide variants. (**A**) Induction of α-helix structure of peptide variants by SDS as monitored by far-UV CD spectroscopy. Peptides TRX 94-108 (○), L94A (Δ), L99A (▼), L103A (□), L107A (■) and NHP (●). (**B**) Urea unfolding of SDS/peptide clusters followed by far-UV CD spectroscopy. Supramolecular clusters were prepared in 5.0 m*M* SDS. In all cases peptide concentrations were 100 μ*M*, the buffer was 2.0 m*M* sodium phosphate, pH 7.0. All experiments were performed at 25°C.

Capillary zone electrophoresis uncovers SDS binding to the peptide

To investigate SDS binding to the peptide (and its variants), we explored their behavior by capillary zone electrophoresis (CZE, Fig. 4). In the absence of SDS, the electrophoretic mobility of all peptides is similar to that of the electro-osmotic flow reference compound (acetonitrile), indicating that under this condition (pH 7.0), the net charge of all peptides is zero. However, at 5.0 mM SDS, all peptides show a lower electrophoretic mobility than the neutral reference. This decreased mobility can be accounted for by a concerted change in net negative charge (as a consequence of the binding of SDS molecules) and the size (measured by the R_h) of the supramolecular cluster. The SDS/TRX94-108 cluster shows the lowest mobility among all peptides assayed. By contrast, all mutants show similarly higher mobility, with the exception of NHP that moves the most. At 2.0 mM SDS, detergent molecules bind to TRX94-108, but not to NHP, as judged by its electrophoretic mobility. This difference is also consistent with α-helical induction results (see above). At 2.0 m*M* SDS a significant heterogeneity is revealed by the shape of the electropherogram for TRX94-108, which is also seen for NHP at higher SDS concentrations (5.0 m*M*), probably uncovering the presence of multiple conformations.[26,36] This fact indicates that the latter peptide interacts weakly with the detergent. We suggest that this behavior is consistent with the low hydrophobic moment predicted for NHP (Table I and Supporting Information Fig. S1), linking this molecular property to its tendency to form secondary structure. By using the CZE mobility (-4.36×10^{-8} m^2 V^{-1} s^{-1}) and the R_h (21.2 Å, by DOSY-NMR) in 5.0 m*M* SDS, we were able to calculate a charge for the SDS/TRX94-108 supramolecular cluster that is compatible with 11 ± 1 molecules of SDS per complex.

Interaction with an unspecific apolar surface also stabilizes the helical conformation of peptide TRX94-108

We analyzed the strength of the interaction between a hydrophobic matrix (C18 RP-HPLC resin) and peptide variants. Retention times of random coil peptides are expected to be significantly different from those determined for α-helical peptides.[37] This is probably the con-

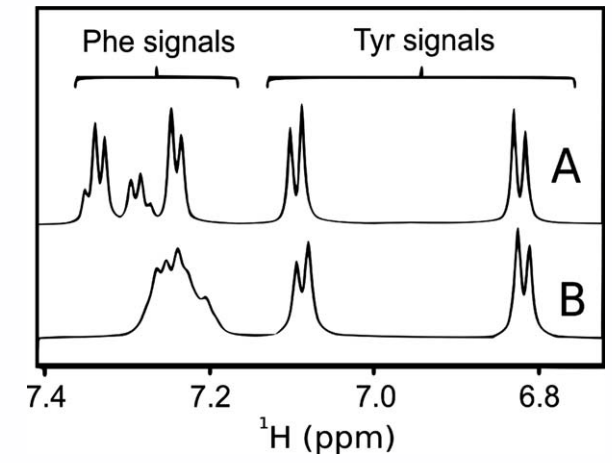

Figure 3

^{1}H NMR spectra of aromatic side chains of TRX94-108 in the absence of SDS (**A**) or containing 5.0 m*M* SDS (**B**). Buffer was 2.0 m*M* sodium phosphate, pH 7.0. Peptide concentration was 200 μ*M*. Spectra were registered at 25°C in D_2O.

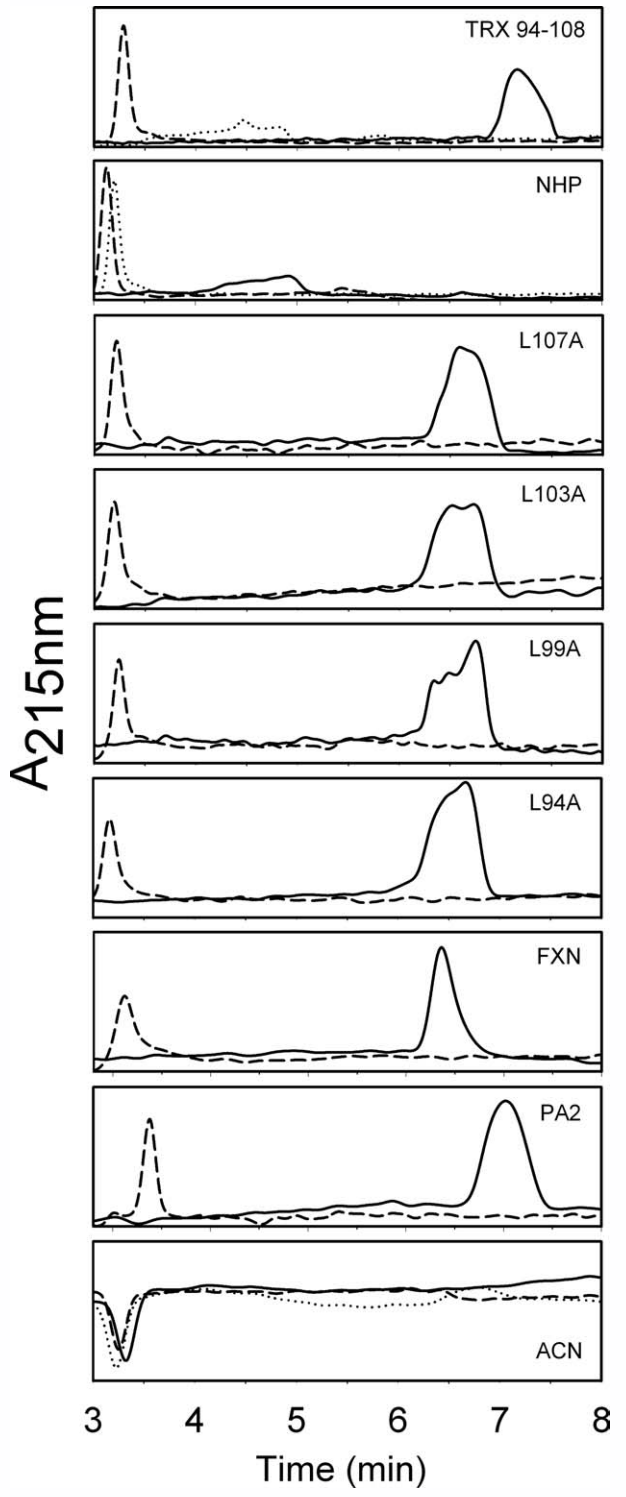

Figure 4

Capillary Zone Electrophoresis of peptide variants. Peptides were run in 0.0 m*M* (– –) and in 5.0 m*M* SDS (——); for TRX94-108 and NHP additional runs in the presence of 2.0 m*M* SDS were also performed (·····). In all cases, peptide concentration was 100 μ*M* and buffer was 2.0 m*M* sodium phosphate, pH 7.0. All experiments were carried out at 25°C. ACN was used as the electro-osmotic neutral reference (bottom box).

sequence of reducing the energetic cost of partitioning peptide bonds involved in hydrogen bonding into an apolar environment, as shown by Ladokhin *et al.*[38] In this context, a single amino acid substitution could bear an effect on α-helical propensity, hydrophobicity and stability. Although overall hydrophobicity is the driving force that determines peptide binding, secondary structure propensity is able to tune it as well.[39] The retention profiles for all peptides assayed are shown in Figure 5(A). TRX94-108 elutes with the largest retention time. It is particularly revealing that L107A and L94A mutants, which are less hydrophobic than NHP, elute at higher ACN concentrations. On the other hand, L99A and L103A elute at lower concentrations of ACN than peptides L107A and L94A. It is noteworthy that these variants share the same amino acid composition, therefore the same hydrophobicity. These results strongly suggest the existence of a correlation between binding/retention of peptides to the C18 matrix and helical propensity. This effect is much more pronounced when comparing the behavior of wild-type and NHP [Fig. 5(A)]. In addition, to evaluate whether TRX94-108 binds to the C18 surface in a helical conformation, we modified quartz plates with C18-alkyl chains, as described by Blondelle *et al.*[21] and analyzed the secondary structure of bound peptide by CD spectroscopy. Clearly, the far-UV CD spectrum of TRX94-108 bound to the C18 surface matches the typical α-helical signatures, whereas bound NHP shows a spectrum compatible with predominantly unstructured conformations [Fig. 5(B)].

SDS induces α-helical conformation in other amphipathic peptides

We also performed experiments to assess whether the detergent-induced formation of helical structure occurs for other amphipathic peptides unrelated to TRX94-108. For this task we selected two amphipathic helical segments corresponding to a pair of very different proteins: human frataxin, a nuclear-encoded mitochondrial protein whose deficit is the main cause of Friedreich's ataxia,[40] and *Archaeoglobus fulgidus* CopA, one of the few helical membrane proteins for which reversible unfolding has been demonstrated.[41] Similarly to TRX94-108, these two peptides: FXN H2 (residues 181–195 from frataxin) and PA2 (residues 312–326 from CopA) are unstructured in solution, but acquire α-helical conformation in the presence of SDS [Fig. 1(B)]. In 5.0 m*M* SDS solution, peptide FXN H2 shows a far-UV CD signal compatible with ∼50% full helical content, whereas peptide PA2 reaches a signal close to 100% helix. In addition, the electropherograms of both peptides show gain of negative charge as a consequence of SDS binding (see Fig. 4). It is noteworthy that the amphipathic character of peptide FXN H2 (μ_H = 7.67) resembles that of TRX94-108 (Table 1), mainly due to the location of four leucine residues in a row in the folded

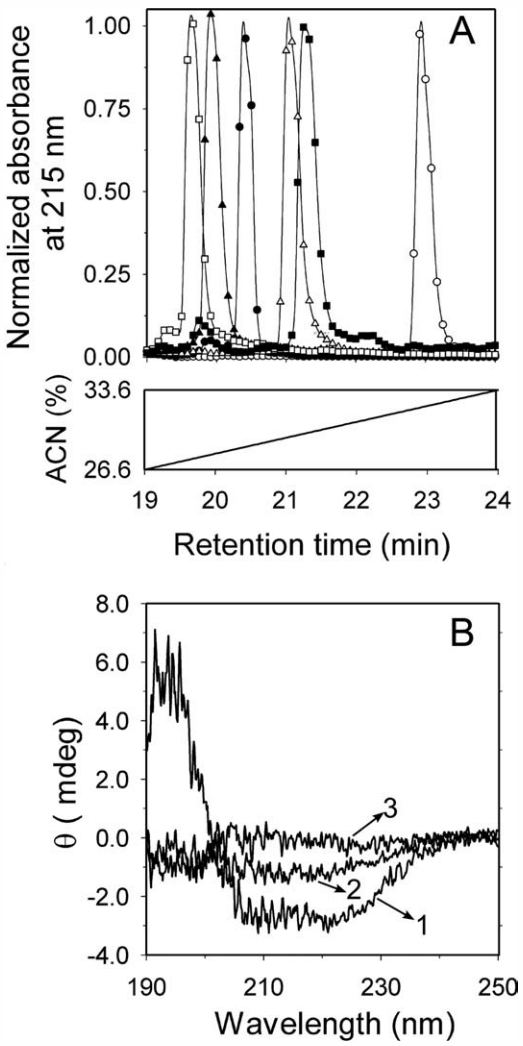

Figure 5

Induction of α-helix structure by C18 hydrophobic surfaces. (**A**) RP-HPLC retention time of TRX94-108 (○), NHP (●), L94A (Δ), L99A (▲), L103A (□), and L107A (■). Peptides at 10 μ*M* were eluted with a 5.0 m*M* sodium phosphate, pH 7.0/ACN gradient that ranged from 0 to 42% ACN in 30 min. Standard deviation ($n = 3$) in retention times is 11 s. Peptides were followed by absorbance at 215 nm. The ACN gradient corresponding to the retention time of the peptide variants (19–24%) is shown. (**B**) CD spectra corresponding to the bound peptides to C18 modified quartz plates TRX 94-108,[1] NHP,[2] and the spectrum of quartz plates after removing peptide with isopropanol between experiments.[3]

conformation (Supporting Information Fig. S3). On the other hand, PA2—bearing no sequence identity with TRX94-108—is also remarkably amphipathic ($\mu_H = 8.73$).

Molecular dynamics reveal the nature of the interaction between TRX94-108 and SDS

To investigate the α-helix stabilization process, we studied the interaction between TRX94-108 and SDS molecules by MDS. The simulations show that in all cases, along the first few nanoseconds SDS molecules interact with the apolar face of the peptide and reside there for the rest of the simulation (see Fig. 6).

Interestingly, in all cases corresponding to SDS:peptide molar ratios equal or above 3:1, residues 96–103 (KGQLKEFL) conserve the starting α-helical conformation during the entire simulation (Fig. 6, for a detailed description see the Ramachandran plots in Supporting Information Fig. S2). Thus, ∼50% of the peptide structure (8 out of 15 residues) remains in helical conformation when complexed to SDS. Moreover, C-terminal residues 104–108 (DANLA), which also start in helical structure, unwind in the first few nanoseconds of the simulation. The only exception was one of the simulations involving six SDS molecules, where the C-terminal moiety refolds. All these results correlate well with the helical induction effect of SDS observed by far-UV CD.

As we previously suggested, MDS reveal that L107 is in an unstructured region and that this leucine does not establish strong interactions with the helical region of the peptide (Fig. 7 and Supporting Information Fig. S2). Thus, this result reveals why the L107A mutation bears only a minor effect on the stability of α-helical structure when compared with L99A or L103A. In this sense, the analysis of inter atomic distances in the course of the simulations indicates that L103–L107 side chains are outside the boundaries of van der Waals interaction [interatomic distances: >8 Å and >10 Å, for C_β-C_β and C_γ-C_γ, respectively: Fig. 7(C,D)]. By contrast, this analysis also shows that L94 and L99 are roughly at van der Waals distances [inter atomic distances: (5 Å and (6 Å, for C_β-C_β and C_γ-C_γ, respectively: Fig. 7(C,D)]. The same closeness is observed for residues L99 and L103. Thus, in solution L94 interacts with the hydrophobic face of helical part of the peptide and, probably, this interaction slightly stabilizes the α-helical structure through leucine stacking (L94-L99-L103), explaining the observed reduction in helical propensity for L94A [Fig. 2(A)]. Interestingly, this orientation of L94 is remarkably similar to that adopted by this residue in the context of the native structure of the protein (PDB ID: 2TRX).

On the other hand, when MDS were run in the absence of SDS molecules, the helical conformation is completely lost (within the first 10–20 ns) and distances between neighboring leucine residues are >10 Å apart, with the exception of the pair L94–L99 [Figs. 7(A,B)], which remains at van der Waals distance.

The analysis of SDS to peptide distances using the radial distribution functions $G(r)$ shows that SDS molecules mainly interact through their carbon tails with the apolar amino acid side chains [Fig. 8(E)]. Particularly relevant seems to be the interaction between detergent molecules and side chains of L94, L99, and L103. In addition, we observed electrostatic interactions involving

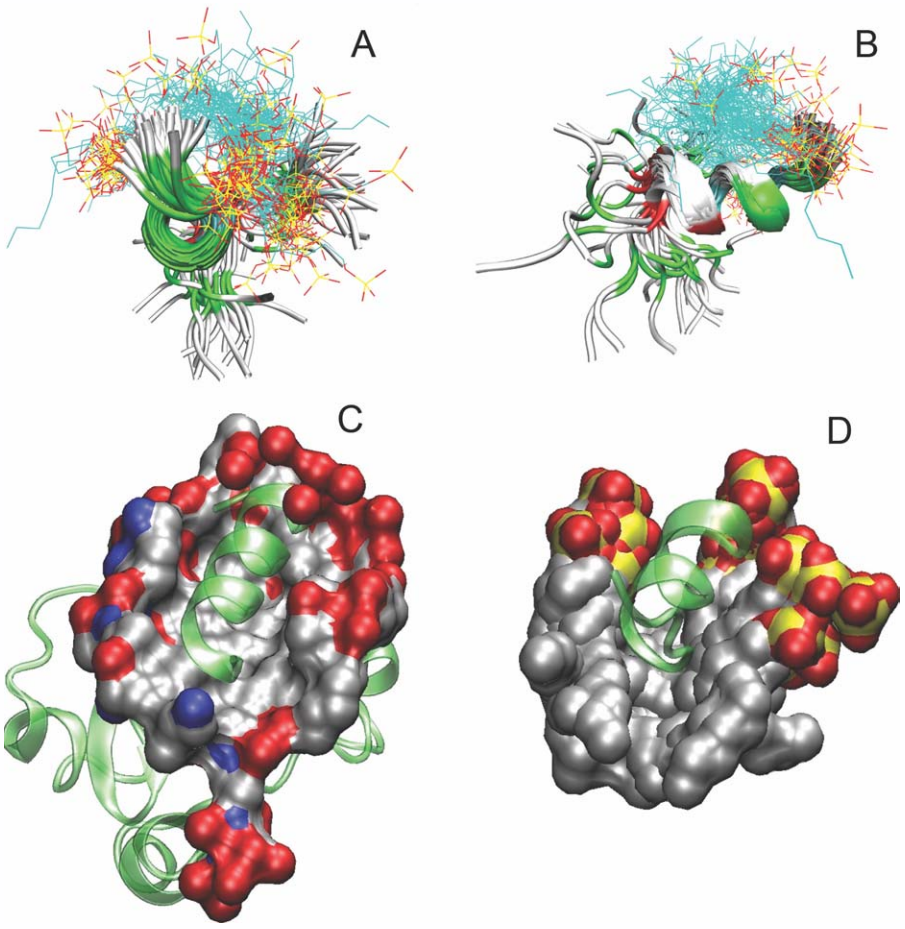

Figure 6

MDS of SDS/TRX94-108 supramolecular cluster. Representative structures of the SDS/TRX94-108 cluster along the simulation with three SDS molecules. (**A**) Ribbon diagram models of 20 superimposed TRX94-108/SDS structures. The peptide is colored by residue type: polar (green), basic (blue), acidic (red), apolar (white). SDS molecules are represented as sticks (apolar carbon tail in cyan and sulfate group in red and yellow (oxygen, sulfur atoms respectively). (**B**) Rear view of (A) which results from a 90 rotation of the left view around a horizontal axis. (**C**) Van der Waals surface of the close environment (colored by atom type) of residues 94–108 (in ribbon) in 2TRX structure. (**D**) Van der Waals surface model of SDS molecules of 20 representative snap-shots during the MDS colored by atom type and in ribbon a representative structure of peptide TRX94-108.

SDS sulfate groups and the ε amino group of K96 or the HN of S95 [Fig. 7(F)].

Significantly, when the SDS:peptide molar ratio is 2:1 or 1:1, MDS show that SDS molecules still bind to the peptide surface. However, in these cases the helical structure is not preserved. This indicates that there is a critical number of SDS molecules needed to stabilize the α-helix structure of the peptide.

To understand why the SPS molecules do not induce α-helical conformation, as evidenced by CD spectroscopy, we ran MDS of TRX94-108 in the presence of SPS molecules (4:1, 6:1, and 8:1 molar ratios). We observed that these molecules interact weakly with the peptide and do not preserve the starting helical structure. Thus, the helix unwinds similarly to the MDS without SDS. These simulations support the idea that the hydrocarbon tail length can be considered a key factor in the stabilization of secondary structure mediated by hydrophobic interactions, which is in agreement with the experimental results shown above [Fig. 1(B)].

DISCUSSION

Acquisition of the helical conformation of TRX94-108 does not depend on the specific structure of a protein counterpart

In this work, we studied how an essentially unstructured peptide acquires a native-like conformation. Experimental work presented here demonstrates that TRX94-108, a moderately amphipathic peptide of the surface of the globular protein thioredoxin, from *E. coli*, folds into a helical structure upon binding to SDS or C18-alkyl-modified surfaces, as shown by CD, CZE, and RP-HPLC. The local apolar environment provided by detergent mol-

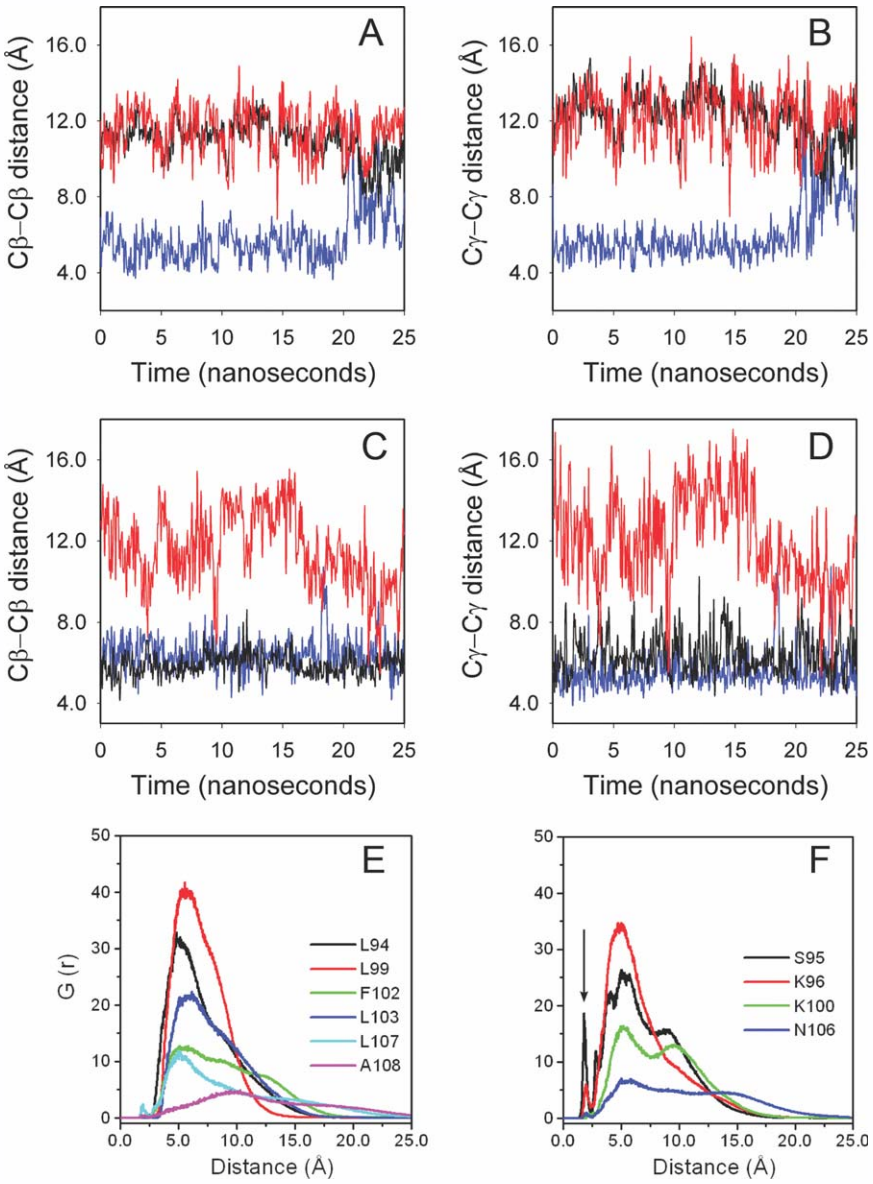

Figure 7

Interatomic distances between Cβ-Cβ or Cγ-Cγ of neighbor leucine residues were calculated along the simulation: L94–L99 (blue line), L99–L103 (black line), and L103–L107 (red line). MDS were performed in the absence (**A** and **B**) and in the presence of three SDS molecules per peptide (**C** and **D**). The radial distribution function, $G(r)$, for selected apolar (**E**) and polar (**F**) residues of TRX94-108 obtained from MDS (SDS:peptide 3:1 molar ratio). The black arrow points to H-bond interactions.

ecules or alkyl chains is sufficient to induce and stabilize the structure of the peptide. This behavior was extensively described earlier for other peptide systems,[5,21,39,42] including peptide-chaperone interaction[43] and interaction between amphipathic peptides and membranes.[44,45] However, analysis at the atomic level by MDS presented here highlights the picture of the peptide/detergent complex, suggesting that stabilization of the helical structure results from the existence of key contact points given by a critical number of SDS molecules interacting with particular hydrophobic side chains. Moreover, experiments with site-specific mutants of the peptide show that the induction and stability of secondary structure is highly tuned by amino acid residues located at the center of the peptide (L99 and L103).

A dynamic structural scaffold serves to stabilize the native conformation of peptide TRX94-108

In essence, MDS analysis puts forward the notion that at least three SDS molecules are needed to stabilize a

supramolecular cluster with α-helical secondary structure. We suggest that the dynamic apolar surface formed by SDS molecules [Fig. 6(D)] serves as a structural scaffold to induce—or select—the native conformation of a module which would otherwise be unstructured in aqueous solution. Thus, a relevant question arises about which structural elements provide the scaffold for residues 94 to 108 in TRX folding. Cumulative evidence in the field points to a context dominated by a "β floor" for this purpose. In this regard, it was demonstrated for *E. coli* TRX that early folding events yield a burst intermediate (BI) characterized by the presence of local hydrophobic clusters. This intermediate detected along refolding is rich in β and devoid of α structure (α = 6%, β = 36%, when compared with the native state: α = 40%, β = 30%).[46] Furthermore, by using a complementation system based on the interaction between three TRX fragments, Tasayco *et al.* showed that the initiation site for folding may comprise strands β2 and β4, and that the interaction between these two elements would constitute the first folding event.[47] In this direction, Bhutani *et al.* demonstrated by native-state hydrogen-exchange experiments that the unfolded state of TRX contains residual β structure.[48] Taken together, these results suggest that the stabilization of α-helical structure along TRX folding would take place after the formation of the β core. Nevertheless, by using the complementation system TRX1-93/TRX94-108 we showed that full consolidation of tertiary structure leading to the re-establishment of a functional thioredoxin fold also depends on the interaction of key residues belonging to α helix 3.[13] Remarkably, despite the complexities of the native interaction surface [Fig. 6(C)], the dynamic picture arising from the SDS contacts mimics the former reasonably well [Fig. 6(D)].

Interaction between structural modules and apolar surfaces in collapsed conformations could represent a general folding step

The fact that folding of TRX94-108 does not require a cognate structure with a preformed tightly-packed core suggests that folding might be thought of as a sequential process. After an initial hydrophobic collapse, secondary structure stabilization based on its interaction with apolar surfaces occurs, followed by steps where specific tertiary contacts contribute to consolidate the native state. In this context, our results rationalize the existence of folding intermediates in the TRX folding process.[46] The accumulation of intermediate states may depend on how the nonspecific interaction rounds are coordinated with the subsequent tertiary structure consolidation. In one extreme (full synergy) the nucleation-condensation mechanism would take place via the formation of a weakly structured local nucleus with simultaneous cooperative formation of extended tertiary structure. In the other extreme, the diffusion-collision mechanism (partial synergy) would dominate, with the presence of non-native interactions, rapid formation of individual nuclei (in general including secondary structure elements) followed by docking to achieve consolidation, thus giving rise to a more rugged energy landscape. In both cases, the modular organization of proteins would simplify the search of the conformational space.

ACKNOWLEDGMENTS

The authors thank Dr. Mauricio Sica for useful discussions; Mr. Andrés Binolfi and Dr. Claudio Fernández for assistance with NMR experiments; Ms. Mariana Hamer and Dr. Irene Rezzano for their help with chemical modification of quartz surfaces; and Ms. Romina Monasterio and Dr. Nora Vizzioli for assistance in CZE experiments.

REFERENCES

1. Anfinsen CB. Principles that govern the folding of protein chains. Science 1973;181:223–230.
2. Risso VA, Primo ME, Ermácora MR. Re-engineering a beta-lactamase using prototype peptides from a library of local structural motifs. Protein Sci 2009;18:440–449.
3. Mohanraja K, Dhanasekaran M, Kundu B, Durani S. Mechanism-based protein design: attempted "nucleation-condensation" approach to a possible minimal helix-bundle protein. Biopolymers 2003;70:355–363.
4. Hill RB, Raleigh DP, Lombardi A, DeGrado WF. De novo design of helical bundles as models for understanding protein folding and function. Acc Chem Res 2000;33:745–754.
5. Hodges RS, Zhu BY, Zhou NE, Mant CT. Reversed-phase liquid chromatography as a useful probe of hydrophobic interactions involved in protein folding and protein stability. J Chromatogr A 1994;676:3–15.
6. Montserret R, McLeish MJ, Bockmann A, Geourjon C, Penin F. Involvement of electrostatic interactions in the mechanism of peptide folding induced by sodium dodecyl sulfate binding. Biochemistry 2000;39:8362–8373.
7. Luo P, Baldwin RL. Mechanism of helix induction by trifluoroethanol: a framework for extrapolating the helix-forming properties of peptides from trifluoroethanol/water mixtures back to water. Biochemistry 1997;36:8413–8421.
8. Roccatano D, Colombo G, Fioroni M, Mark AE. Mechanism by which 2,2,2-trifluoroethanol/water mixtures stabilize secondary-structure formation in peptides: a molecular dynamics study. Proc Natl Acad Sci USA 2002;99:12179–12184.
9. Andersen KK, Otzen DE. How chain length and charge affect surfactant denaturation of acyl coenzyme A binding protein (ACBP). J Phys Chem B 2009;113:13942–13952.
10. Najbar LV, Craik DJ, Wade JD, McLeish MJ. Identification of initiation sites for T4 lysozyme folding using CD and NMR spectroscopy of peptide fragments. Biochemistry 2000;39:5911–5920.
11. Parker W, Song PS. Protein structures in SDS micelle-protein complexes. Biophys J 1992;61:1435–1439.
12. Santos J, Marino-Buslje C, Kleinman C, Ermacora MR, Delfino JM. Consolidation of the thioredoxin fold by peptide recognition: interaction between *E. coli* thioredoxin fragments 1–93 and 94–108. Biochemistry 2007;46:5148–5159.
13. Santos J, Sica MP, Buslje CM, Garrote AM, Ermacora MR, Delfino JM. Structural selection of a native fold by peptide recognition. Insights into the thioredoxin folding mechanism. Biochemistry 2009;48:595–607.
14. Muñóz V, Serrano L. Elucidating the folding problem of helical peptides using empirical parameters. Nat Struct Biol 1994;1:399–409.

15. Muñóz V, Serrano L. Elucidating the folding problem of helical peptides using empirical parameters. II. Helix macrodipole effects and rational modification of the helical content of natural peptides. J Mol Biol 1995;245:275–296.
16. Muñóz V, Serrano L. Elucidating the folding problem of helical peptides using empirical parameters. III. Temperature and pH dependence. J Mol Biol 1995;245:297–308.
17. Petukhov M, Muñóz V, Yumoto N, Yoshikawa S, Serrano L. Position dependence of non-polar amino acid intrinsic helical propensities. J Mol Biol 1998;278:279–289.
18. Fauchere JL, Charton M, Kier LB, Verloop A, Pliska V. Amino acid side chain parameters for correlation studies in biology and pharmacology. Int J Pept Protein Res 1988;32:269–278.
19. Dhe-Paganon S, Shigeta R, Chi YI, Ristow M, Shoelson SE. Crystal structure of human frataxin. J Biol Chem 2000;275:30753–30756.
20. Sazinsky MH, Agarwal S, Arguello JM, Rosenzweig AC. Structure of the actuator domain from the *Archaeoglobus fulgidus* Cu(+)-ATPase. Biochemistry 2006;45:9949–9955.
21. Blondelle SE, Ostresh JM, Houghten RA, Perez-Paya E. Induced conformational states of amphipathic peptides in aqueous/lipid environments. Biophys J 1995;68:351–359.
22. Reynolds JA, Tanford C. Binding of dodecyl sulfate to proteins at high binding ratios. Possible implications for the state of proteins in biological membranes Proc Natl Acad Sci USA 1970;66:1002–1007.
23. da Graca Miguel M, Eidelman O, Ollivon M, Walter A. Temperature dependence of the vesicle-micelle transition of egg phosphatidylcholine and octyl glucoside. Biochemistry 1989;28:8921–8928.
24. Kosower EM, Dodiuk H, Tanizawa K, Ottolenghi M, Orbachl N. Intramolecular donor-acceptor systems. radiative and nonradiative processes for the excited states of 2-N-arylamino-6-naphthalenesulfonates. J Am Chem Soc 1975;97:2167–2177.
25. Kosower EM, Kanety H. Intramolecular donor-acceptor systems. 10. Multiple fluorescences from 8-(phenylamino) 1 - naphthalenesulfonates J Am Chem Soc 1983;105:6236–6246.
26. Schneider GF, Shaw BF, Lee A, Carillho E, Whitesides GM. Pathway for unfolding of ubiquitin in sodium dodecyl sulfate, studied by capillary electrophoresis. J Am Chem Soc 2008;130:17384–17393.
27. Winzor DJ, Jones S, Harding SE. Determination of protein charge by capillary zone electrophoresis. Anal Biochem 2004;333:225–229.
28. Wilkins DK, Grimshaw SB, Receveur V, Dobson CM, Jones JA, Smith LJ. Hydrodynamic radii of native and denatured proteins measured by pulse field gradient NMR techniques. Biochemistry 1999;38:16424–16431.
29. Van Der Spoel D, Lindahl E, Hess B, Groenhof G, Mark AE, Berendsen HJ. GROMACS: fast, flexible, and free. J Comput Chem 2005;26:1701–1718.
30. Oostenbrink C, Villa A, Mark AE, van Gunsteren WF. A biomolecular force field based on the free enthalpy of hydration and solvation: the GROMOS force-field parameter sets 53A5 and 53A6. J Comput Chem 2004;25:1656–1676.
31. van Aalten DM, Bywater R, Findlay JB, Hendlich M, Hooft RW, Vriend G. PRODRG, a program for generating molecular topologies and unique molecular descriptors from coordinates of small molecules. J Comput Aided Mol Des 1996;10:255–262.
32. Berendsen HJC, Postma JPM, Gunsteren WFv, DiNola A, Haak JR. Molecular dynamics with coupling to an external bath. J Chem Phys 1984;81:3684–3690.
33. Katti SK, LeMaster DM, Eklund H. Crystal structure of thioredoxin from Escherichia coli at 1.68 A resolution. J Mol Biol 1990;212:167–184.
34. Berendsen HJC, Grigera JR, Straatsma TP. The missing term in effective pair potentials. J Chem Phys 2002;91:6269–6271.
35. Humphrey W, Dalke A, Schulten K. VMD: visual molecular dynamics. J Mol Graph 1996;14:33–38;27–28.
36. Stutz H, Wallner M, Malissa H, Jr, Bordin G, Rodriguez AR. Detection of coexisting protein conformations in capillary zone electrophoresis subsequent to transient contact with sodium dodecyl sulfate solutions. Electrophoresis 2005;26:1089–1105.
37. Mant CT, Kovacs JM, Kim HM, Pollock DD, Hodges RS. Intrinsic amino acid side-chain hydrophilicity/hydrophobicity coefficients determined by reversed-phase high-performance liquid chromatography of model peptides: comparison with other hydrophilicity/hydrophobicity scales. Biopolymers 2009;92:573–595.
38. Ladokhin AS, White SH. Folding of amphipathic alpha-helices on membranes: energetics of helix formation by melittin. J Mol Biol 1999;285:1363–1369.
39. Wieprecht T, Rothemund S, Bienert M, Krause E. Role of helix formation for the retention of peptides in reversed-phase high-performance liquid chromatography. J Chromatogr A 2001;912:1–12.
40. Rai M, Soragni E, Chou CJ, Barnes G, Jones S, Rusche JR, Gottesfeld JM, Pandolfo M. Two new pimelic diphenylamide HDAC inhibitors induce sustained frataxin upregulation in cells from Friedreich's ataxia patients and in a mouse model. PLoS One 2010;5:e8825.
41. Roman EA, Arguello JM, Gonzalez Flecha FL. Reversible unfolding of a thermophilic membrane protein in phospholipid/detergent mixed micelles. J Mol Biol 2010;397:550–559.
42. Chen Y, Mant CT, Hodges RS. Temperature selectivity effects in reversed-phase liquid chromatography due to conformation differences between helical and non-helical peptides. J Chromatogr A 2003;1010:45–61.
43. Li Y, Gao X, Chen L. GroEL recognizes an amphipathic helix and binds to the hydrophobic side. J Biol Chem 2009;284:4324–4331.
44. Houston ME, Jr, Kondejewski LH, Karunaratne DN, Gough M, Fidai S, Hodges RS, Hancock RE. Influence of preformed alpha-helix and alpha-helix induction on the activity of cationic antimicrobial peptides. J Pept Res 1998;52:81–88.
45. Sivakamasundari C, Nagaraj R. Interaction of 18-residue peptides derived from amphipathic helical segments of globular proteins with model membranes. J Biosci 2009;34:239–250.
46. Georgescu RE, Li JH, Goldberg ME, Tasayco ML, Chaffotte AF. Proline isomerization-independent accumulation of an early intermediate and heterogeneity of the folding pathways of a mixed alpha/beta protein. *Escherichia coli* thioredoxin. Biochemistry 1998;37:10286–10297.
47. Tasayco ML, Fuchs J, Yang XM, Dyalram D, Georgescu RE. Interaction between two discontiguous chain segments from the beta-sheet of *Escherichia coli* thioredoxin suggests an initiation site for folding. Biochemistry 2000;39:10613–10618.
48. Bhutani N, Udgaonkar JB. Folding subdomains of thioredoxin characterized by native-state hydrogen exchange. Protein Sci 2003;12:1719–1731.